On Optimizing Feedback Interval for Gauss-Markov MIMO Channels With Finite-Rate Feedback

Kritsada Mamat and Wiroonsak Santipach, *Senior Member, IEEE*

arXiv:1703.03499v1 [cs.IT] 10 Mar 2017

Abstract

Assuming perfect channel state information (CSI), a receiver in a point-to-point MIMO channel can compute the transmit beamforming vector that maximizes the transmission rate. For frequency-division duplex, a transmitter is not able to estimate CSI directly and has to obtain a quantized transmit beamforming vector from the receiver via a rate-limited feedback channel. We assume that time evolution of MIMO channels is modeled as a Gauss-Markov process parameterized by a temporal-correlation coefficient. For a given feedback rate, we analyze the optimal feedback interval that maximizes the average transmission rate or received power of systems with two transmit and/or two receive antennas. For other system sizes, we derive the rate gain in a large system limit, which is shown to approximate the rate gain of a finite-size system well. We find that quantizing transmit beamforming with the optimal feedback interval gives a larger rate than the existing Kalman-filter scheme does by as much as 10%.

Index Terms

MIMO, transmit beamforming, temporal correlated channels, Gauss-Markov process, finite-rate feedback, RVQ, feedback interval.

I. Introduction

Employing multiple antennas at transmitters and/or receivers has been shown to increase spatial diversity and spectral efficiency [2], [3]. To gain the full potential of multiple antennas,

This work was supported by postdoctoral funding from the Faculty of Engineering, Kasetsart University, Bangkok, Thailand under grant number 59/02/EE and by the Kasetsart University Research and Development Institute (KURDI) under the FY2018 Kasetsart University research grant.

The material in this paper was presented in part at the IEEE Global Communications Conference (GLOBECOM), Houston, Texas, USA, Dec. 2011 [1].

The authors are with the Department of Electrical Engineering; Faculty of Engineering; Kasetsart University, Bangkok, 10900, Thailand (email: mkritsada1@gmail.com; wiroonsak.s@ku.ac.th).

channel state information (CSI) at both the transmitter and receiver is required. At a receiver, CSI can be estimated from pilot signals. However, estimating the channel at a transmitter is not possible for frequency-division duplex (FDD) where the forward and backward channels are in different frequency bands. Consequently, a transmitter in FDD must obtain CSI from a receiver via a low-rate feedback channel. Many researchers have proposed schemes to quantize and feed back CSI and analyze the associated performance (see [4] and references therein). In our work, we assume that the receiver has perfect CSI and thus, can compute the optimal transmit beamforming vector that maximizes an instantaneous achievable rate. Imperfect CSI at the receiver in conjunction with limited feedback has been considered in our previous work [5]. With finite feedback rate , the beamforming vector is selected from a quantization set or a codebook, which is known *a priori* at the transmitter and the receiver. The codebook index of the selected vector is then fed back to the transmitter, which subsequently adjusts its beamforming coefficients accordingly. Different codebooks have been proposed and analyzed in [4], [6]–[8].

Feeding back quantized beamforming coefficients may not be useful in a fast fading channel since they are quickly outdated [9]. If the channel fades slowly, the beamforming coefficients may not need to be updated frequently. Thus, the feedback scheme should be adapted to temporal correlation of the channel [10]–[15]. Switched codebook quantization was proposed in [10] where the codebook selection was based on channel spatial and temporal correlations. In [11], the authors proposed a polar-cap differential codebook, which rotates according to the current time instant to quantize the beamforming vector in multiple-input and single-output (MISO) channels. In [12], quantized CSI was modeled as a first-order finite-state Markov chain and beamforming feedback is based on the channel dynamics. An adaptive feedback period (AFP) scheme in which the transmitter feeds back to the receiver periodically was considered in [13]. However, the authors were only concerned with MISO channels in which the number of receive antennas is fixed to 1. In our work here, we also consider the same AFP scheme, but with MIMO channels whose analysis is more complex. For [13] and this work, the frequency of feedback update is determined by temporal correlation of the channel. The optimal feedback period for coordinated multi-point systems was considered in [14] where channels are also modeled as a first-order Gauss-Markov process. In [15], the minimum feedback rate of a differential feedback scheme was analyzed.

Another line of work [16]–[18] applied Kalman filter (KF) to predict the current transmission channel based on previous estimates and channel correlation. References [16], [17] proposed quantizing and feeding back an innovation term, which is the difference between

the received signal and its estimate, to the transmitter. The current channel estimate then can be computed by the transmitter using KF with a sequence of the previous quantized innovations. In [17], only 2 bits per update was required to send back innovations and was used to compute the beamforming vector by the transmitter. CSI at the receiver was obtained via a pilot signal and was not perfect. Reference [18] improved the training phase of KF beamforming in massive MIMO systems by reducing the amount of pilot.

For this work, we consider block fading MIMO channel with time evolution modeled by a first-order Gauss-Markov process. We analyze the performance of quantized beamforming in the AFP scheme first proposed by [13], which considered only MISO channels. In our previous work [19], we also considered quantizing transmit beamforming in MISO channels, but in conjunction with orthogonal frequency-division multiplexing (OFDM), and optimize the size of subcarrier cluster . To quantize transmit beamforming, we apply random vector quantization (RVQ) codebook, which has been shown to perform close to the optimum codebook [6], [20]. Furthermore, RVQ can be analyzed to obtain some insights into the limited feedback performance. We would like to determine the optimal feedback interval of the AFP scheme.

First we derive closed-form expressions of the averaged received power for channels with either two transmit or two receive antennas and formulate the problems that find the optimal feedback interval. For channels with an arbitrary number of antennas, we derive the averaged rate gain in a large system limit in which the numbers of transmit and receive antennas and the number of feedback bits tend to infinity with fixed ratios. Numerical examples show that the large system results can be used to approximate the optimal feedback interval of finite-size systems. (Some analytical and simulation results of the large system in this work have been presented in [1].) Finally, we compare the rate performance for a given feedback rate of several feedback schemes and find that the AFP scheme with the optimal feedback interval outperforms a minimum feedback-period (MFP) scheme, which updates feedback for every fading block, especially in a low-feedback rate regime. The AFP scheme also outperforms KF beamforming with quantized innovation and the performance gain can be significant in MIMO channels.

The paper is organized as follows. Section II introduces the channel model and feedback schemes. In Section III, we analyze the optimal feedback interval for systems with two transmit and/or two receive antennas. Large system analysis is shown in Section IV. The numerical results and conclusions are in Sections V and VI, respectively.

II. System Model

We consider a point-to-point discrete-time multiantenna channel with N_t transmit and N_r receive antennas. We assume block fading in which the channel gains remain static for L symbols and change in the next block of symbols. To allow meaningful feedback of CSI from a receiver, the block length L, which is also a coherence period, is assumed to be sufficiently long. During the kth fading block, an $N_r \times 1$ receive vector during symbol index $kL + l$ is given by

$$\boldsymbol{r}(kL + l) = \boldsymbol{H}(k)\boldsymbol{v}(k)x_s(kL + l) + \boldsymbol{n}(kL + l), \quad 1 \leq l \leq L \tag{1}$$

where $x_s(i)$ is the ith transmitted symbol with zero mean and unit variance, $\boldsymbol{n}(i)$ is an $N_r \times 1$ additive white Gaussian noise (AWGN) vector during symbol index i with zero mean and covariance $\sigma_n^2 \boldsymbol{I}$ where $\boldsymbol{I}$ is an identity matrix, $\boldsymbol{v}(k)$ is an $N_t \times 1$ unit-norm beamforming vector for the kth fading block, and $\boldsymbol{H}(k) = [h_{ij}(k)]$ is an $N_r \times N_t$ channel matrix whose element $h_{ij}(k)$ is the channel gain between the ith transmit and the jth receive antennas during the kth fading block. Here, we consider rank-one transmit precoding or beamforming. Arbitrary-rank transmit precoding with multiple independent data streams was considered in [6]. Assuming an ideal scattering environment, $h_{ij}(k)$ is modeled as a complex Gaussian random variable with zero mean and unit variance. Also, we assume that adjacent antennas in antenna arrays at both the transmitter and receiver are placed sufficiently far apart that elements of $\boldsymbol{H}(k)$ are independent.

To model a time evolution of the channel considered, we adopt the first-order Gauss-Markov process, which has been widely used and was shown to predict channel dynamics well [10], [13], [21], [22]. Thus, the channel matrix of the kth fading block relates to that of the previous block as follows

$$\boldsymbol{H}(k) = \alpha \boldsymbol{H}(k-1) + \sqrt{1-\alpha^2}\boldsymbol{W}(k) \tag{2}$$

where $\boldsymbol{W}(k)$ is an $N_r \times N_t$ innovation matrix with independent zero-mean unit-variance complex Gaussian entries, and $\alpha \in [0, 1]$ denotes a temporal correlation coefficient between adjacent blocks. Note that $\alpha = 1$ produces a time-invariant channel. On the other hand, $\alpha = 0$ indicates a channel with no temporal correlation and thus, the channel fades independently from one coherence block to the next.[1]

[1]For the Jakes/Clarke fading model [23], $\alpha = \mathbb{J}_0(2\pi D_s T_s)$ where $\mathbb{J}_0(\cdot)$ is the zeroth-order Bessel function, D_s is the Doppler spread, and T_s is the sampling time.

The associated ergodic achievable rate of this channel is given by

$$R = E\left[\log\left(1 + \rho \boldsymbol{v}(k)^\dagger \boldsymbol{H}(k)^\dagger \boldsymbol{H}(k)\boldsymbol{v}(k)\right)\right] \tag{3}$$

where $\rho = 1/\sigma_n^2$ denotes the background signal-to-noise ratio (SNR) and the expectation is over channel matrix and beamforming vector. To achieve the desired rate, the transmitter encodes the transmitted symbols across many different fading blocks. In addition to SNR, the achievable rate also depends on the beamforming vector $\boldsymbol{v}(k)$. If the transmitter can track the channel perfectly (perfect CSI), the optimal $\boldsymbol{v}(k)$ is the eigenvector of the channel covariance $\boldsymbol{H}(k)^\dagger \boldsymbol{H}(k)$ corresponding to the maximum eigenvalue. In other words, the optimal beamforming vector is in the direction of the strongest channel mode.

With FDD, the transmitter is not able to estimate the channel directly and has to rely on CSI fed back from the receiver via a rate-limited channel. The receiver can estimate the channel from pilot signals, which is known *a priori* at the transmitter and receiver. Assuming perfect CSI, the receiver selects the optimal beamforming vector and sends it back via a feedback channel to the transmitter. Since the feedback channel is rate-limited, the selected beamforming vector needs to be quantized. Here, we quantize the transmit beamforming vector with a random vector quantization (RVQ) codebook

$$\mathcal{V} = \{\boldsymbol{v}_1, \boldsymbol{v}_2, \cdots, \boldsymbol{v}_n\} \tag{4}$$

where entries $\boldsymbol{v}_j$ are independent isotropically distributed and n denotes the number of entries in the RVQ codebook. For given $B_q = \log_2 n$ feedback bits for quantization, RVQ performs close to the optimal codebook [6], [20] and RVQ is optimal (i.e. maximizes achievable rate) in a large system limit [6], [24] to be defined.

Given B_q bits and channel matrix $\boldsymbol{H}(k)$, the receiver selects from the RVQ codebook

$$\hat{\boldsymbol{v}}(k) = \arg\max_{\boldsymbol{v}_j \in \mathcal{V}} \ \log\left(1 + \rho \boldsymbol{v}_j^\dagger \boldsymbol{H}(k)^\dagger \boldsymbol{H}(k)\boldsymbol{v}_j\right) \tag{5}$$

$$= \arg\max_{\boldsymbol{v}_j \in \mathcal{V}} \ \boldsymbol{v}_j^\dagger \boldsymbol{H}(k)^\dagger \boldsymbol{H}(k)\boldsymbol{v}_j. \tag{6}$$

The index of the selected beamforming vector is then fed back to the transmitter, which adjusts its beamforming vector accordingly. We assume that the time duration to feed back the selected index is negligible when compared to one fading block and that the feedback channel is error-free. The associated achievable rate with a quantized transmit beamformer is given by

$$R = E\left[\log\left(1 + \rho \hat{\boldsymbol{v}}(k)^\dagger \boldsymbol{H}(k)^\dagger \boldsymbol{H}(k)\hat{\boldsymbol{v}}(k)\right)\right]. \tag{7}$$

Since the channel is time-varying, the transmit beamforming needs to be quantized and fed back for every fading block. This may not be practical due to the limited feedback rate. However, the system can take an advantage of the temporal correlation in order to reduce the number of bits needed. In this paper, we consider feedback schemes that reduce the number of feedback bits while maintaining performance.

III. On Optimizing Feedback Interval

Suppose that there are B feedback bits available per one fading block. Since the overhead must be kept small, B bits per fading block may not be sufficient to meaningfully quantize a beamforming vector $\boldsymbol{v}$. In the AFP scheme proposed by [13], $\boldsymbol{v}$ is quantized and fed back at the beginning of every interval of K fading blocks with BK bits instead of every block with B bits. However, the transmit beamforming vector quantized to the first fading block with more feedback bits will gradually be outdated as time passes. Thus, the feedback interval K should be adjusted to the temporal correlation of the channel. In this section, we analyze the optimal feedback interval for MIMO channels in the AFP scheme. Note that the feedback interval was analyzed for MISO channels by [13].

First, we determine an average achievable rate over K fading blocks given by

$$\bar{R} = \frac{1}{K}\sum_{k=1}^{K} E\left[\log\left(1+\rho\hat{\boldsymbol{v}}(1)^{\dagger}\boldsymbol{H}(k)^{\dagger}\boldsymbol{H}(k)\hat{\boldsymbol{v}}(1)\right)\right] \tag{8}$$

$$\leq \log\left(1+\rho\frac{1}{K}\sum_{k=1}^{K} E\left[\hat{\boldsymbol{v}}(1)^{\dagger}\boldsymbol{H}(k)^{\dagger}\boldsymbol{H}(k)\hat{\boldsymbol{v}}(1)\right]\right) \tag{9}$$

where $\hat{\boldsymbol{v}}(1)$ is the quantized transmit beamformer for the channel $\boldsymbol{H}(1)$ in the first fading block and we apply Jensen's inequality to obtain the upper bound (9). From (8), we see that for the AFP scheme, the quantized beamformer of the first block is used for all K consecutive blocks. Since the expression of the average rate in (8) is not tractable, we choose to instead maximize the rate upper bound in (9) and obtain the feedback interval as follows

$$K^{*} = \arg\max_{K\in\mathbb{Z}^{+}} \frac{1}{K}\sum_{k=1}^{K} E\left[\hat{\boldsymbol{v}}(1)^{\dagger}\boldsymbol{H}(k)^{\dagger}\boldsymbol{H}(k)\hat{\boldsymbol{v}}(1)\right], \tag{10}$$

which is an integer optimization problem. The problem in (10) is to maximize the average received power over K blocks. If K is not too large, an exhaustive search can be performed to find the optimal feedback interval K^{*}.

A. 2×2 *Channels*

For a point-to-point channel with two transmit and two receive antennas, the following lemma gives the expected received power during the kth fading block when the quantized transmit beamforming for the first block is used.

Lemma 1: Given that $N_t = 2$, $N_r = 2$, and the number of bits to quantize $\boldsymbol{v}(1)$ is BK,

$$E\left[\hat{\boldsymbol{v}}(1)^\dagger \boldsymbol{H}(k)^\dagger \boldsymbol{H}(k)\hat{\boldsymbol{v}}(1)\right] = \alpha^{2k-2}\left(1.5 - \frac{3}{2^{BK}+1}\right) + 2, \quad \forall k \geq 1. \tag{11}$$

The proof is in Appendix A.

We see that as k increases, the received power decreases since the channel becomes less matched to the transmit beamformer $\hat{\boldsymbol{v}}(1)$. However, if the channel is highly correlated (α close to 1), the received power will gradually decrease with time. Averaged over K fading blocks with B bits per fading block, the received power for 2×2 channels is given by

$$\frac{1}{K}\sum_{k=1}^{K} E\left[\hat{\boldsymbol{v}}(1)^\dagger \boldsymbol{H}(k)^\dagger \boldsymbol{H}(k)\hat{\boldsymbol{v}}(1)\right] = \frac{1}{K}\left(1.5 - \frac{3}{2^{BK}+1}\right)\left(\frac{1-\alpha^{2K}}{1-\alpha^2}\right) + 2. \tag{12}$$

We note that the average received power increases with B. To determine K^* that maximizes the average received power, we substitute (12) into (10) and solve the problem.

In [13], the performance of the AFP scheme is compared with that of the minimum feedback period (MFP) scheme in which transmit beamforming is quantized and fed back to the transmitter for every fading block ($K = 1$). For a given feedback rate of B bits per fading block, the AFP scheme (with $K > 1$) outperforms the MFP scheme (with $K = 1$) if

$$\frac{1}{K}\left(1.5 - \frac{3}{2^{BK}+1}\right)\left(\frac{1-\alpha^{2K}}{1-\alpha^2}\right) + 2 > 3.5 - \frac{3}{2^B+1} \tag{13}$$

where the right-hand side of (13) is the average received power in (12) with $K = 1$. With some algebraic manipulation, we obtain

$$K < \frac{(1-\alpha^{2K})(2^B+1)(2^{BK}-1)}{(1-\alpha^2)(2^B-1)(2^{BK}+1)} < \left(\frac{1}{1-\alpha^2}\right)\left(\frac{2^B+1}{2^B-1}\right). \tag{14}$$

The above inequality implies that the maximum feedback interval of the AFP scheme that outperforms the MFP scheme depends largely on the temporal correlation α and less on the feedback rate B, especially when B is large. The feedback interval for the AFP scheme can be set larger when channels are less correlated and should be shortened when channels are highly correlated.

B. $2 \times N_r$ *Channels*

We extend the previous analysis to channels with $N_r \geq 2$. For example, the receiver could be a base station, which can operate a large number of receive antennas. We first evaluate the received power of the first fading block when BK feedback bits are available, and obtain the following.

Lemma 2: For $2 \times N_r$ channels with $N_r \geq 2$ and BK feedback bits,

$$\gamma_{2\times N_r}(BK) \triangleq E\left[\hat{\boldsymbol{v}}(1)^\dagger \boldsymbol{H}(1)^\dagger \boldsymbol{H}(1)\hat{\boldsymbol{v}}(1)\right] \tag{15}$$

$$\begin{aligned} &= \frac{1}{(N_r-1)!(N_r-2)!}\Big[\phi(N_r+2, N_r-1) - 2\phi(N_r+1, N_r) \\ &\quad + \phi(N_r, N_r+1) - \frac{1}{2^{BK}+1}\big(\phi(N_r+2, N_r-1) \\ &\quad - 3\phi(N_r+1, N_r) + 3\phi(N_r, N_r+1) - \phi(N_r-1, N_r+2)\big)\Big] \end{aligned} \tag{16}$$

where $\phi(m, n)$ is a recursive function given by

$$\phi(m,n) = mn\phi(m-1, n-1) - \frac{(m-n)(m+n-1)!}{2^{m+n+1}}, \quad \forall m, n \geq 1 \tag{17}$$

with the following initial conditions: $\phi(4,1) = \frac{45}{8}$, $\phi(3,2) = \frac{11}{8}$, $\phi(2,3) = \frac{5}{8}$, and $\phi(1,4) = \frac{3}{8}$. The proof is in Appendix B.

The received power for the kth block of a $2 \times N_r$ channel can be analyzed similarly to that of a 2×2 channel. Applying (53) and (61) in Appendix A, we can show that

$$E\left[\hat{\boldsymbol{v}}(1)^\dagger \boldsymbol{H}(k)^\dagger \boldsymbol{H}(k)\hat{\boldsymbol{v}}(1)\right] = \alpha^{2k-2}\left(\gamma_{2\times N_r}(BK) - N_r\right) + N_r. \tag{18}$$

Averaged over the whole feedback interval, the received power for a $2 \times N_r$ channel is given by

$$\frac{1}{K}\sum_{k=1}^{K} E\left[\hat{\boldsymbol{v}}^\dagger(1)\boldsymbol{H}^\dagger(k)\boldsymbol{H}(k)\hat{\boldsymbol{v}}(1)\right] = N_r + \frac{1}{K}\left(\frac{1-\alpha^{2K}}{1-\alpha^2}\right)\left(\gamma_{2\times N_r}(BK) - N_r\right). \tag{19}$$

Similar to a 2×2 channel, we obtain the optimal feedback interval K^* by solving (10) with the expression of the received power from (19).

We remark that with $K = 1$, the average received power equals $\gamma_{2\times N_r}(B)$, which is also the received power of the MFP scheme. To find the maximum feedback interval where the AFP scheme outperforms the MFP one, we solve the following inequality

$$N_r + \frac{1}{K}\left(\frac{1-\alpha^{2K}}{1-\alpha^2}\right)\left(\gamma_{2\times N_r}(BK) - N_r\right) > \gamma_{2\times N_r}(B). \tag{20}$$

Thus,

$$K < \left(\frac{1-\alpha^{2K}}{1-\alpha^2}\right)\left(\frac{\gamma_{2\times N_r}(BK) - N_r}{\gamma_{2\times N_r}(B) - N_r}\right) < \frac{1}{1-\alpha^2}\left(\frac{\gamma_{2\times N_r}(BK) - N_r}{\gamma_{2\times N_r}(B) - N_r}\right). \tag{21}$$

Since $\gamma_{2\times N_r}(BK) \approx \gamma_{2\times N_r}(B)$ for a large feedback rate B, a similar remark pertaining to 2×2 channels N_r can be made here. The maximum feedback interval for the AFP scheme depends significantly on α and less on B or the number of receive antennas N_r when B is large.

C. $N_t \times 2$ Channels

Next, we consider channels with $N_t > 2$ transmit antennas and two receive antennas. The results are applicable to a downlink in which the base station can have a large number of transmit antennas. We can follow the derivation of the averaged received power for $2 \times N_r$ channels in Section III-B to obtain the averaged received power for $N_t \times 2$ channels,

$$\frac{1}{K}\sum_{k=1}^{K} E\left[\hat{\boldsymbol{v}}^{\dagger}(1)\boldsymbol{H}^{\dagger}(k)\boldsymbol{H}(k)\hat{\boldsymbol{v}}(1)\right] = 2 + \frac{1}{K}\left(\frac{1-\alpha^{2K}}{1-\alpha^2}\right)\left(\gamma_{N_t\times 2}(BK) - 2\right) \tag{22}$$

where the above expression follows (19) with $N_r = 2$, and

$$\gamma_{N_t\times 2}(BK) = E\left[\hat{\boldsymbol{v}}(1)^{\dagger}\boldsymbol{H}(1)^{\dagger}\boldsymbol{H}(1)\hat{\boldsymbol{v}}(1)\right] \tag{23}$$

is the received power of the first block. Recall that

$$\hat{\boldsymbol{v}}(1)^{\dagger}\boldsymbol{H}(1)^{\dagger}\boldsymbol{H}(1)\hat{\boldsymbol{v}}(1) = \max_{1\le j\le 2^{BK}} \boldsymbol{v}_j^{\dagger}\boldsymbol{H}(1)^{\dagger}\boldsymbol{H}(1)\boldsymbol{v}_j. \tag{24}$$

Since the RVQ codebook is employed, the probability density function (pdf) of $\boldsymbol{v}_j^{\dagger}\boldsymbol{H}(1)^{\dagger}\boldsymbol{H}(1)\boldsymbol{v}_j$ is identical for all j and is equal to $\boldsymbol{v}_j^{\dagger}\boldsymbol{\Lambda}\boldsymbol{v}_j$ [25] where $\boldsymbol{\Lambda}$ is an $N_t \times N_t$ diagonal matrix whose main diagonal entries are the ordered eigenvalues of $\boldsymbol{H}(1)^{\dagger}\boldsymbol{H}(1)$. For this channel, there are only two nonzero eigenvalues, which are denoted by λ_1 and λ_2 and $\lambda_1 \ge \lambda_2 > 0$. We derive the distribution of $\boldsymbol{v}_j^{\dagger}\boldsymbol{\Lambda}\boldsymbol{v}_j$ and obtain the following lemma.

Lemma 3:

Let $\boldsymbol{v}$ be an $N_t \times 1$ isotropically distributed vector and $\boldsymbol{\Lambda} = \mathrm{diag}([\lambda_1, \lambda_2, \underbrace{0, 0, ..., 0}_{N_t-2}])$ with $\lambda_1 \ge \lambda_2 > 0$. The cumulative distribution function (cdf) of $\boldsymbol{v}^{\dagger}\boldsymbol{\Lambda}\boldsymbol{v}$ conditioned on λ_1 and λ_2 is given by

$$F_{\boldsymbol{v}^{\dagger}\boldsymbol{\Lambda}\boldsymbol{v}|\lambda_1,\lambda_2}(x) = \begin{cases} 1 - \frac{\lambda_1}{\lambda_1-\lambda_2}\left(1-\frac{x}{\lambda_1}\right)^{N_t-1} + \frac{\lambda_2}{\lambda_1-\lambda_2}\left(1-\frac{x}{\lambda_2}\right)^{N_t-1} & : \quad 0 \le x \le \lambda_2 \\ 1 - \frac{(\lambda_1-x)^{N_t-1}}{(\lambda_1-\lambda_2)\lambda_1^{N_t-2}} & : \quad \lambda_2 \le x \le \lambda_1. \end{cases} \tag{25}$$

The proof is shown in Appendix C.

With (24) and (25), it is straightforward to show that

$$E\left[\hat{\boldsymbol{v}}(1)^{\dagger}\boldsymbol{H}(1)^{\dagger}\boldsymbol{H}(1)\hat{\boldsymbol{v}}(1)|\lambda_1,\lambda_2\right] = \lambda_1 - \int_0^{\lambda_1} \left(F_{\boldsymbol{v}^{\dagger}\boldsymbol{\Lambda}\boldsymbol{v}}(x)\right)^{2^{BK}} \mathrm{d}x. \tag{26}$$

Thus,

$$E\left[\hat{\boldsymbol{v}}(1)^{\dagger}\boldsymbol{H}(1)^{\dagger}\boldsymbol{H}(1)\hat{\boldsymbol{v}}(1)\right]=\int_{0}^{\infty}\int_{0}^{\lambda_1}E\left[\hat{\boldsymbol{v}}(1)^{\dagger}\boldsymbol{H}(1)^{\dagger}\boldsymbol{H}(1)\hat{\boldsymbol{v}}(1)|\lambda_1,\lambda_2\right]f_{\boldsymbol{\Lambda}}(\lambda_1,\lambda_2)\,\mathrm{d}\lambda_1\mathrm{d}\lambda_2 \tag{27}$$

where $f_{\boldsymbol{\Lambda}}(\lambda_1,\lambda_2)$ is the joint pdf of the two ordered eigenvalues of $\boldsymbol{H}(1)^{\dagger}\boldsymbol{H}(1)$ and is stated in (63) where N_t replaces N_r. Substitute (26) into (27) and evaluate the first integral to obtain

$$\gamma_{N_t\times 2}(BK)=\frac{\phi(N_t+2,N_t-1)}{(N_t-1)!(N_t-2)!}-\int_{0}^{\infty}\int_{0}^{\lambda_1}\int_{0}^{\lambda_1}\left(F_{\boldsymbol{v}^{\dagger}\boldsymbol{\Lambda}\boldsymbol{v}}(x)\right)^{2^{BK}}f_{\boldsymbol{\Lambda}}(\lambda_1,\lambda_2)\,\mathrm{d}x\,\mathrm{d}\lambda_1\mathrm{d}\lambda_2. \tag{28}$$

The recursive function ϕ is defined in (17). The integral in (28) can be evaluated by any numerical method. We remark that the expression for the average received power in (28) does not apply for $N_t=2$ since the cdf derived in Lemma 3 only applies when $N_t>2$. We find the optimal feedback interval K^* by maximizing the average received power in (22), which is determined by (22) and (28). The same conclusion made for the previous two channel models on the maximum feedback interval of the AFP scheme still applies for this channel model. However, [6] has shown that in order to maintain $\gamma_{N_t\times 2}$, B needs to scale with N_t as N_t becomes large. Hence, for a fixed feedback rate, the maximum feedback interval of the AFP scheme will decrease as N_t increases.

For channels with arbitrary N_t and N_r, the expression for the received power is not tractable due to the pdf of $\boldsymbol{v}^{\dagger}\boldsymbol{\Lambda}\boldsymbol{v}$ and the joint pdf of the ordered eigenvalues of $\boldsymbol{H}(1)^{\dagger}\boldsymbol{H}(1)$. However, the performance of the system with an arbitrary number of antennas can be well approximated by its performance in a large system regime to be defined in the next section.

IV. Large System Analysis

The large system limit refers to one in which N_t, N_r, B tend to infinity with fixed $\bar{N}_r \triangleq N_r/N_t$ and $\bar{B}\triangleq B/N_t$. In a large system limit, the pdf of the ordered eigenvalues converges to a deterministic function [26] and hence, performance analysis of systems with arbitrary size becomes accessible. It is shown by [6] that with some feedback ($\bar{B}>0$) and fixed $\bar{N}_r$, the achievable rate defined in (7) increases with $\log(\rho N_t)$. Thus, we define an achievable rate gain as follows

$$R_{\triangle}\triangleq R-\log(\rho N_t) \tag{29}$$

$$=E\left[\log\left(\frac{1}{\rho N_t}+\frac{1}{N_t}\hat{\boldsymbol{v}}(k)^{\dagger}\boldsymbol{H}(k)^{\dagger}\boldsymbol{H}(k)\hat{\boldsymbol{v}}(k)\right)\right]. \tag{30}$$

With feedback rate $\bar{B}$ per fading block, we apply the AFP scheme described in Section III and compute the average rate gain over an interval of K fading blocks given by

$$\bar{R}_{\triangle} = \frac{1}{K}\sum_{k=1}^{K} E\left[\log\left(\frac{1}{\rho N_t} + \frac{1}{N_t}\hat{\boldsymbol{v}}(1)^{\dagger}\boldsymbol{H}(k)^{\dagger}\boldsymbol{H}(k)\hat{\boldsymbol{v}}(1)\right)\right] \tag{31}$$

where the quantized beamforming of the first block is used for the whole interval of K blocks. We note that in the previous section, we chose to evaluate the upper bound on the rate via the average received power due to the intractability of the rate analysis. However, in this section, we evaluate the rate directly.

A. Large System With $\bar{N}_r > 0$

First we consider the large system with $\bar{N}_r > 0$. In other words, the numbers of transmit and receive antennas are increasing at the same rate. Similar to the analysis of the system with a finite number of antennas, we determine the received power per transmit antenna $\frac{1}{N_t}\hat{\boldsymbol{v}}^{\dagger}(1)\boldsymbol{H}^{\dagger}(k)\boldsymbol{H}(k)\hat{\boldsymbol{v}}(1)$ by applying the Gauss-Markov equation in (2) and evaluate each term after substitution. The first of the two nonzero terms is shown by [6], [24] to converge in a large system limit

$$\frac{1}{N_t}\hat{\boldsymbol{v}}(1)^{\dagger}\boldsymbol{H}(1)^{\dagger}\boldsymbol{H}(1)\hat{\boldsymbol{v}}(1) \longrightarrow \gamma_{\infty}\left(\bar{B}K\right) \tag{32}$$

where $\bar{B}K$ is the normalized feedback bits used for quantizing $\hat{\boldsymbol{v}}(1)$ and the expression for the function $\gamma_{\infty}(x)$ is as follows [6]. Suppose

$$\beta = \frac{1}{\log(2)}\left(\bar{N}_r \log\left(\frac{\sqrt{\bar{N}_r}}{1+\sqrt{\bar{N}_r}}\right) + \sqrt{\bar{N}_r}\right). \tag{33}$$

For $0 \le x \le \beta$, γ_{∞} satisfies

$$(\gamma_{\infty})^{\bar{N}_r}\,\mathrm{e}^{-\gamma_{\infty}} = 2^{-x}\left(\frac{\bar{N}_r}{\mathrm{e}}\right)^{\bar{N}_r} \tag{34}$$

and for $x \ge \beta$,

$$\gamma_{\infty}(x) = (1+\sqrt{\bar{N}_r})^2 - \exp\Big\{\frac{1}{2}\bar{N}_r\log(\bar{N}_r) - (\bar{N}_r - 1)\log(1+\sqrt{\bar{N}_r}) + \sqrt{\bar{N}_r} - x\log(2)\Big\}. \tag{35}$$

The second nonzero term can be shown to converge to

$$\frac{1}{N_t}\hat{\boldsymbol{v}}(1)^{\dagger}\boldsymbol{W}(k-i)^{\dagger}\boldsymbol{W}(k-i)\hat{\boldsymbol{v}}(1) \longrightarrow \bar{N}_r. \tag{36}$$

Applying (32) and (36), we obtain

$$\lim_{(N_t,N_r,B)\to\infty}\frac{1}{N_t}\hat{\boldsymbol{v}}(1)^{\dagger}\boldsymbol{H}(k)^{\dagger}\boldsymbol{H}(k)\hat{\boldsymbol{v}}(1) = \bar{N}_r + \alpha^{2k-2}\left(\gamma_{\infty}\left(\bar{B}K\right) - \bar{N}_r\right). \tag{37}$$

Consequently, the expression for the asymptotic rate gain is given by

$$\bar{R}_{\triangle}^{\infty} = \lim_{(N_t,N_r,B)\to\infty} \bar{R}_{\triangle} \tag{38}$$

$$= \frac{1}{K}\sum_{k=1}^{K} \log(\bar{N}_r + \alpha^{2k-2}\left(\gamma_{\infty}\left(\bar{B}K\right) - \bar{N}_r\right)). \tag{39}$$

We would like to maximize the asymptotic achievable rate gain averaged over the feedback interval K. For a given feedback rate of $\bar{B}$ and $\bar{N}_r > 0$, the optimal feedback interval that maximizes the asymptotic achievable rate gain is therefore given by

$$K^* = \arg\max_{K\in\mathbb{Z}^+} \left[\prod_{k=1}^{K} \bar{N}_r + \alpha^{2(k-1)}\left(\gamma_{\infty}\left(\bar{B}K\right) - \bar{N}_r\right)\right]^{\frac{1}{K}}. \tag{40}$$

Similar to a finite-size system, exhaustive search over some range of K can be used to obtain a suboptimal feedback interval. We note that the optimal feedback interval in (40) will depend on the temporal correlation coefficient, feedback rate, and the number of transmit and receiver antennas. Next we consider two extreme regimes for which $\alpha \to 0$ and $\alpha \to 1$. When the channel does not change ($\alpha \to 1$), the optimal feedback interval K^* can be shown to be infinite from (40). This implies that only one feedback update at the start with all available feedback bits giving the maximum rate gain.

When the channel fades independently from a current block to the next block ($\alpha \to 0$), we can maximize the rate-gain expression in (39) over K and obtain

$$K^* = \arg\max_{K\in\mathbb{Z}^+} \frac{1}{K}\log\left(\frac{\gamma_{\infty}(\bar{B}K)}{\bar{N}_r}\right). \tag{41}$$

We remark that for moderate to large $\bar{B}$, $K^* = 1$. Hence, if the channel is temporally uncorrelated, the feedback update must be as frequent as possible. In other words, the MFP scheme will outperform the AFP scheme.

For general $\bar{N}_r$ and α, to find the range of K in which the AFP scheme performs better than the MFP scheme, we solve for K

$$\bar{R}_{\triangle}^{\infty} > \bar{R}_{\triangle}^{\infty}\big|_{K=1} = \gamma_{\infty}(\bar{B}). \tag{42}$$

B. Large System With $\bar{N}_r \to 0$

Next we examine the system in which $\bar{N}_r \to 0$ in a large system limit. The results will apply when the receiver is equipped with only single antenna (MISO channel) or a fixed number of antennas or when the number of receive antennas increases at a rate less than that of the transmit antennas.

First we evaluate the large system limit of $\frac{1}{N_t}\hat{\boldsymbol{v}}(1)^\dagger \boldsymbol{H}(k)^\dagger \boldsymbol{H}(k)\hat{\boldsymbol{v}}(1)$. For $\bar{N}_r = 0$, [6] shows that

$$\frac{1}{N_t}\hat{\boldsymbol{v}}(1)^\dagger \boldsymbol{H}(1)^\dagger \boldsymbol{H}(1)\hat{\boldsymbol{v}}(1) \longrightarrow \gamma_\infty\left(\bar{B}K\right) \tag{43}$$

$$= 1 - 2^{-\bar{B}K} \tag{44}$$

while

$$\frac{1}{N_t}\hat{\boldsymbol{v}}(1)^\dagger \boldsymbol{W}(k-i)^\dagger \boldsymbol{W}(k-i)\hat{\boldsymbol{v}}(1) \longrightarrow 0. \tag{45}$$

Thus, the asymptotic achievable rate gain is given by

$$\bar{R}_\triangle^\infty = \frac{1}{K}\sum_{k=1}^{K} \log\left(\alpha^{2k-2}(1-2^{-\bar{B}K})\right) \tag{46}$$

$$= (K-1)\log(\alpha) + \log\left(1-2^{-\bar{B}K}\right) \tag{47}$$

for $0 < \alpha \leq 1$.

Maximizing the asymptotic achievable rate gain in (47) gives the optimal feedback interval as follows

$$K^* = \arg\max_{K\in\mathbb{Z}^+} \ \alpha^{K-1}(1-2^{-\bar{B}K}). \tag{48}$$

If the integer constraint is removed, we can find K^* from the first derivative of $\bar{R}_\triangle^\infty$ in (47) and obtain the following approximation

$$K^* \approx \frac{1}{\bar{B}}\log_2\left(1 + \frac{\bar{B}\log 2}{\log\frac{1}{\alpha}}\right) \tag{49}$$

where $0 < \alpha < 1$. We note that for large feedback $\bar{B}$, K^* is small. The solution implies that the feedback update should occur often when a large number of feedback bits is available. For a small-feedback regime ($\bar{B} \to 0$), K^* is approximated as follows

$$\lim_{\bar{B}\to 0} K^* \approx \frac{\log 2}{\log\frac{1}{\alpha}}. \tag{50}$$

We note that K^* is increasing with α. Thus, we can conclude that with a low feedback rate and a highly correlated channel, the feedback interval should be large or the feedback update should occur less frequently.

Comparing the rates obtained from the AFP and MFP schemes, we find that the feedback interval K for the AFP scheme must be larger than

$$K > 1 + \frac{1}{\log\alpha}\log\left(\frac{1-2^{-\bar{B}}}{1-2^{-\bar{B}K}}\right). \tag{51}$$

Hence, as channels become less correlated (large α), K can be large. This bound is obtained by solving

$$\bar{R}_{\triangle}^{\infty} > \bar{R}_{\triangle}^{\infty}\big|_{K=1} = \log(1 - 2^{-B}) \tag{52}$$

where $\bar{R}_{\triangle}^{\infty}(K)$ is stated in (47).

V. Numerical Results

To illustrate the performance of the considered schemes, Monte Carlo simulation is performed with 3,000 channel realizations. First, we compare the analytical results derived in Section III with the simulation results. Fig. 1 shows the average received power over the feedback interval of the AFP scheme with the feedback interval K. The feedback rate $B = 1$ bit per block and correlation coefficient $\alpha = 0.8$. We have two sets of system sizes. For the first set, N_t is fixed at 2 with various N_r (2×2, 2×3, and 2×4). We see that the analytical result in (19), which is shown with a solid line, perfectly matches with the simulation result, which is shown with circles. For all N_r, the optimal feedback interval K^* is 3. Adding more receive antennas will increase the received power since the receiver can capture more transmitted signal. The AFP scheme with the optimal K ($K = 3$) can outperform the MFP scheme ($K = 1$) by close to 10%. For the second set of system sizes in which $N_r = 2$ and N_t varies (2×2, 3×2, 4×2, and 5×2), the analytical result comes from (12), (22), and (28). We see that the optimal interval K^* increases with N_t since the number of bits (BK) required to quantize the beamforming vector increases with N_t. For a larger system (5×2), the AFP with optimal K can outperform the MFP by as much as 25%.

For 2×2 channels, we see that the AFP scheme with $2 \leq K \leq 7$ gives larger averaged received power than the MFP scheme. The range of K is accurately predicted by (14). For 2×3 and 2×4 channels, the range of K for which the AFP performs better is $2 \leq K \leq 8$, which can be obtained by (21).

Fig. 2 shows the optimal feedback interval K^* for a 2×2 channel for varying the correlation coefficient α and the number of feedback bits per fading block per transmit antenna B/N_t. We see that for a slow fading channel ($\alpha \to 1$), feedback update can be less frequent and thus, the feedback interval is large. On the other hand, fast fading channels (smaller α) require frequent feedback updates. If the feedback rate per transmit antenna (B/N_t) is increased from 0.5 to 1, we see that K^* decreases. From (12), the averaged received power can be increased when K decreases while B increases.

In Fig. 2, we also show the optimal interval K^* of a large system with $\bar{N}_r = 1$ obtained by solving (40). We remark that K^* for a large system is obtained by maximizing the rate

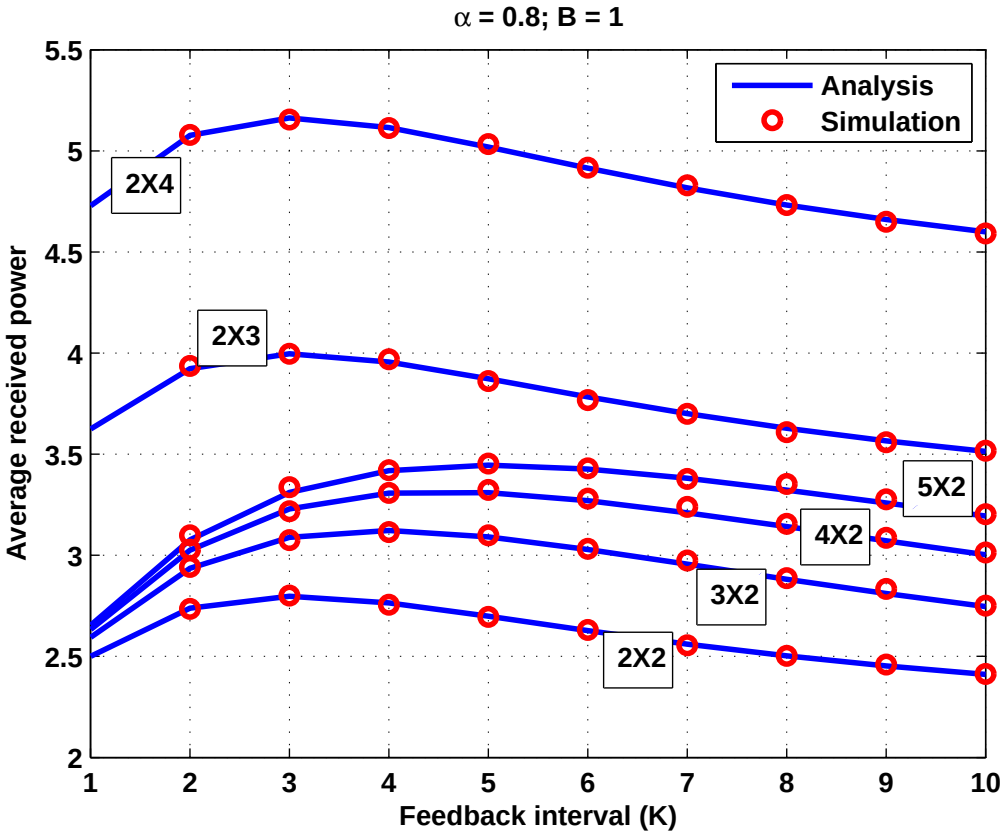

Fig. 1. Received power averaged over the feedback interval is plotted with the length of the feedback interval for various channels where $\alpha = 0.8$ and $B = 1$. Both simulation and analytical results are shown.

gain while K^* for a 2×2 channel is obtained by maximizing the averaged received power. However, we see that the large system results can give a good approximation of those of a very small system.

In Fig. 3, we compare the achievable rate gain of a large system derived in (39) with that of a finite-size system for various feedback rates per transmit antenna $\bar{B}$. The feedback interval K is fixed at 8 blocks and SNR ρ is at 10 dB. The averaged rate gain of finite-size and large systems is obtained from (31) and (39), respectively. We see that as the system size increases from $N_t = 4$ to 8 and 16, the simulation results approach the large system results and that the rate gain increases with $\bar{B}$. However, the rate gain increases at different rates for different α. When the channel is less correlated ($\alpha = 0.5$), the quantized beamforming vector of the first block is not a good substitute for that of the next blocks. Consequently, we do not see much increase in that case although the feedback rate is increased. On the contrary, we see a large increase when the channel is more correlated ($\alpha = 0.9$) since the quantized beamforming vector of the first block performs well for all subsequent blocks in

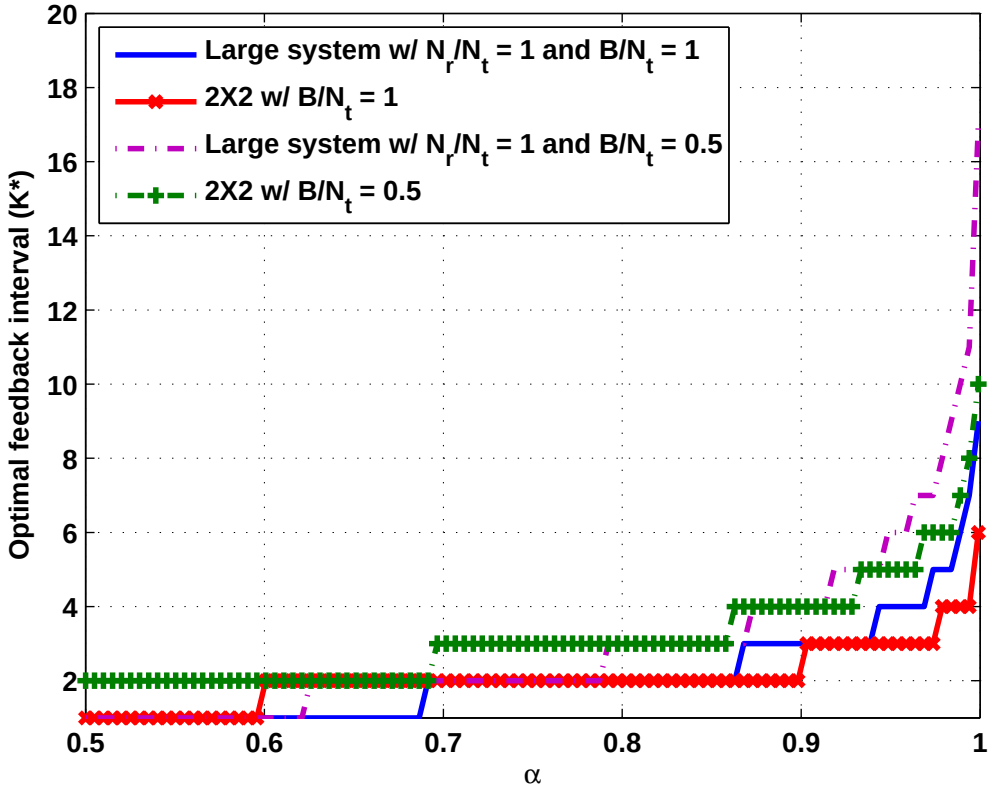

Fig. 2. Optimal feedback intervals for a large system with $\bar{N}_r = 1$ obtained by (40) and for a 2×2 channel obtained by maximizing (12) are shown with varying channel correlation α and feedback rate.

the same interval. Since we quantize beamforming vectors with the RVQ codebook, which requires an exhaustive search to find the quantized vector, the search complexity can be too large for large B. Thus, some of the plots in Fig. 3 do not extend to a larger feedback rate.

In Fig. 4, we set $\bar{B} = 0.25$ and vary K for channels with different temporal correlation. We compare the rate gain of 4×4 channels and that of a large system with $\bar{N}_r = 1$. For a channel with $\alpha = 0.9$, the AFP scheme with $K = 4$ gives a larger rate gain of about 30% more than the MFP scheme does. Although the difference between the results of small-size and large systems is large, the optimal feedback interval K^* obtained from the two results is close. Thus, we can apply the large system analysis to obtain a good approximate for the optimal feedback interval that maximizes the rate gain of a finite-size system. For time-invariant channels ($\alpha = 1$), the optimal K is large.

Fig. 5 shows how the optimal feedback interval K^* increases with the number of transmit antennas N_t, but decreases with the number of feedback bits per fading block B. We set $N_r = 2$ and $\alpha = 0.8$. For larger N_t, the number of bits to quantize the beamforming vector

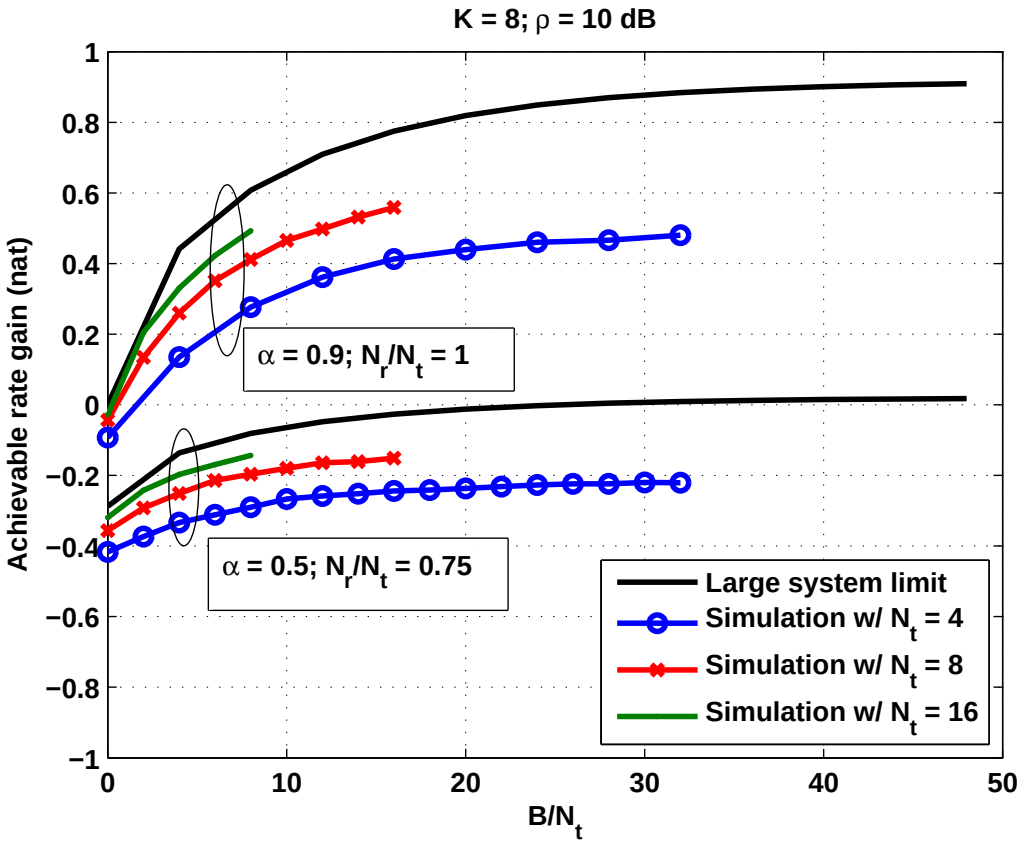

Fig. 3. Averaged rate gain for a large system is compared with that for a finite-size system with $K = 8$ and $\rho = 10$ dB.

needs to increase to maintain the rate performance and hence, the feedback interval has to increase as well. Similar to the results in Fig. 2, as B increases, the feedback interval can be reduced.

In Fig. 6, we compare the AFP and MFP schemes and also the existing KF scheme in the literature for 3×1 and 3×3 channels. In [17], KF is applied to construct the channel vector (or channel matrix) at the transmitter, which then can compute the optimal transmit beamforming. For a fair comparison, we assume that the channel estimation at the receiver is perfect. The receiver quantizes an innovation term, which is the difference between the received signal and its estimate based on channel estimates from previous blocks. The innovation can be straightforwardly shown to be zero-mean Gaussian with some specific variance. Thus, for quantization, we apply a generalized Lloyd algorithm [27], which minimizes the mean square error. The quantized innovation is fed back to the transmitter for every fading block. To construct the channel vector, we follow the steps in [16], [17]. The averaged rate of the KF scheme is shown in Fig. 6.

In Fig. 6, $\alpha = 0.9$ and SNR = 10 dB. We see that the AFP scheme with the optimal K

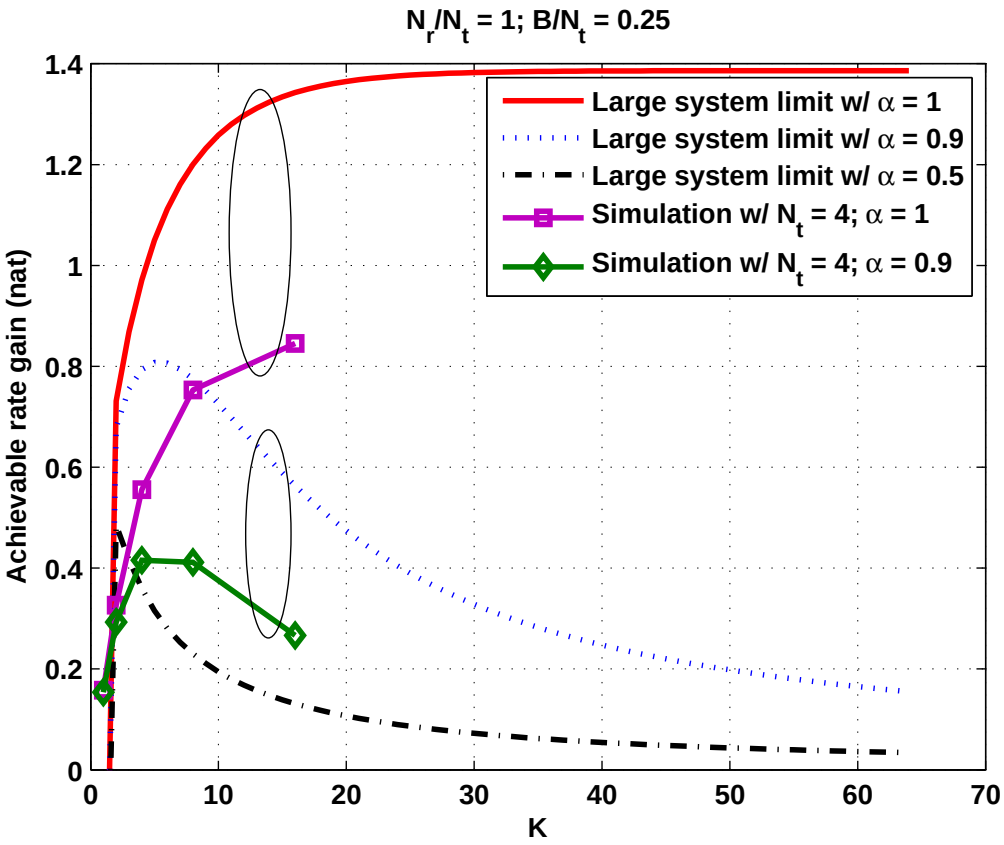

Fig. 4. Averaged rate gain for a large system with $\bar{N}_r = 1$ is compared with that for a 4×4 channel with $\bar{B} = 0.25$ and $\rho = 10$ dB.

performs the best and requires approximately 3 bits per transmit antenna per fading block to achieve close to the optimal beamforming with perfect feedback shown by solid lines in Fig. 6. When the feedback rate is larger than 3 bits per block, $K^* = 1$ and thus, we see that the rate for AFP with K^* and that for MFP is the same. For small to moderate feedback rate, AFP with K^* can perform better than MFP by as much as 10%. We see that the AFP scheme outperforms the KF scheme for all feedback rates for both 3×1 and 3×3 channels. Performance degradation is quite significant for the KF scheme when applied to MIMO channels.

VI. Conclusions

We have analyzed the feedback interval that maximizes the average received power or rate gain for MIMO channels. For the channel model considered, the optimal interval depends more on the channel correlation, the number of transmit antennas, and the feedback rate, and less on the number of receive antennas. For systems with either two transmit or two receive

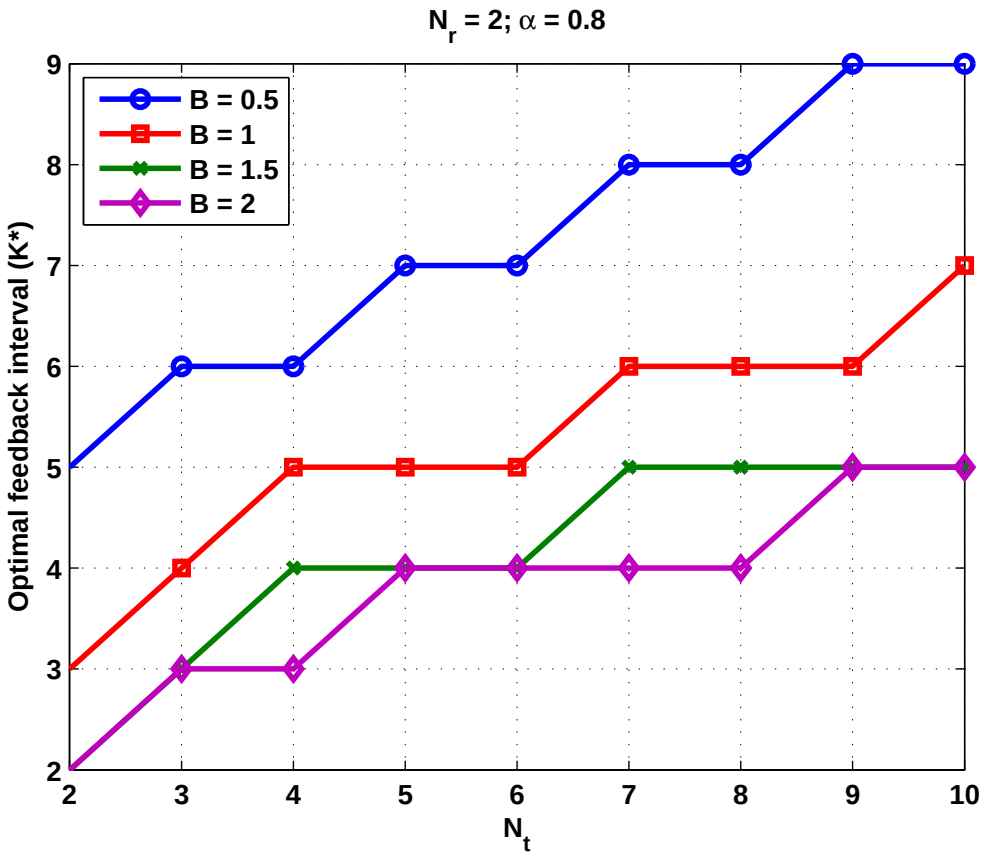

Fig. 5. Optimal feedback intervals K^* for various channel sizes (with fixed $N_r = 2$) are plotted with the number of transmit antennas N_t and the number of feedback bits per fading block B.

antennas, we formulated the received-power maximizing problem in which the exact feedback interval can be found. For systems with other sizes, large system analysis can predict the optimal interval accurately as shown by the numerical examples. When the feedback rate is low, the AFP scheme with the optimal feedback interval outperforms the other schemes including the KF schemes. The performance gain of the AFP scheme over the other schemes can be as much as 10%. Thus, the feedback interval should be adapted according to channel conditions. However, when the feedback rate is high, the performance difference among the different schemes may not be significant.

In this work, we assume that training of the channel is sufficient and thus, CSI at the receiver is perfect. For a system with limited training, the actual performance of the AFP scheme will be lower than that obtained in the paper and the KF scheme may perform better. Since we only consider a point-to-point channel in the present work, broadcast or multiple-access channels are also of interest and can be considered in future work.

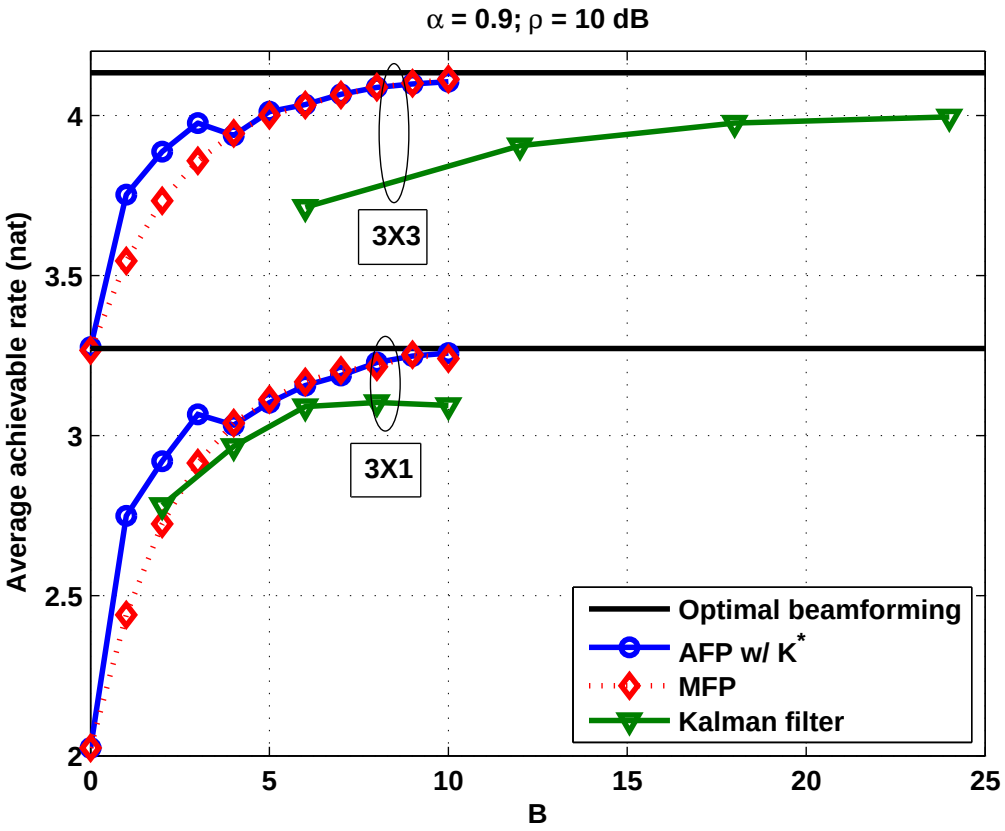

Fig. 6. Average rate of various feedback schemes for 3×1 and 3×3 channels are shown with the number of feedback bits per fading block. $\alpha = 0.9$ and SNR = 10 dB.

APPENDIX

A. *Proof of Lemma 1*

Apply the Gauss-Markov model in (2) and some algebraic manipulation to obtain

$$E\left[\hat{\boldsymbol{v}}(1)^\dagger \boldsymbol{H}(k)^\dagger \boldsymbol{H}(k)\hat{\boldsymbol{v}}(1)\right] = \alpha^{2k-2} E\left[\hat{\boldsymbol{v}}(1)^\dagger \boldsymbol{H}(1)^\dagger \boldsymbol{H}(1)\hat{\boldsymbol{v}}(1)\right] + (1-\alpha^2)\sum_{i=0}^{k-2} \alpha^{2i} E\left[\hat{\boldsymbol{v}}(1)^\dagger \boldsymbol{W}(k-i)^\dagger \boldsymbol{W}(k-i)\hat{\boldsymbol{v}}(1)\right] \quad (53)$$

where the expectation of the cross term that consists of $\boldsymbol{W}$ is equal to zero since $\boldsymbol{W}$ has zero mean and is independent of $\hat{\boldsymbol{v}}(1)$ and all channel matrices $\boldsymbol{H}(k), \forall k$.

We analyze the first expectation in (53). Following the same argument pertaining to the received power in (24), $\boldsymbol{v}_i^\dagger \boldsymbol{H}^\dagger(1)\boldsymbol{H}(1)\boldsymbol{v}_i$ is independent and has the same distribution as $\boldsymbol{v}_i^\dagger \boldsymbol{\Lambda} \boldsymbol{v}_i$ [25] where $\boldsymbol{\Lambda} = \text{diag}([\lambda_1, \lambda_2])$, and λ_1 and λ_2 are the ordered eigenvalues of

$\boldsymbol{H}(1)^\dagger \boldsymbol{H}(1)$ with $\lambda_1 \geq \lambda_2 \geq 0$. The cdf for $\boldsymbol{v}_i^\dagger \boldsymbol{\Lambda} \boldsymbol{v}_i$ conditioned on λ_1 and λ_2 is given by [25]

$$F_{\boldsymbol{v}_i^\dagger \boldsymbol{\Lambda} \boldsymbol{v}_i|\lambda_1,\lambda_2}(x) = \begin{cases} 0 & : \quad 0 \leq x < \lambda_2 \\ \frac{x-\lambda_2}{\lambda_1-\lambda_2} & : \quad \lambda_2 \leq x \leq \lambda_1 \\ 1 & : \quad x > \lambda_1 \end{cases}. \tag{54}$$

We then apply integration by parts to obtain the expression for the conditional expectation as follows

$$E\left[\hat{\boldsymbol{v}}(1)^\dagger \boldsymbol{H}(1)^\dagger \boldsymbol{H}(1) \hat{\boldsymbol{v}}(1) | \lambda_1, \lambda_2\right] = \lambda_1 - \int_{\lambda_2}^{\lambda_1} \left(F_{\boldsymbol{v}_i^\dagger \boldsymbol{\Lambda} \boldsymbol{v}_i|\lambda_1,\lambda_2}(x)\right)^{2^{BK}} \mathrm{d}x \tag{55}$$

$$= \lambda_1 - \frac{\lambda_1 - \lambda_2}{2^{BK}+1}. \tag{56}$$

The joint pdf of the two ordered eigenvalues of $\boldsymbol{H}(1)^\dagger \boldsymbol{H}(1)$, which is a Wishart matrix, is given by [28]

$$f_{\boldsymbol{\Lambda}}(\lambda_1, \lambda_2) = (\lambda_1 - \lambda_2)^2 \mathrm{e}^{-(\lambda_1+\lambda_2)}, \quad \lambda_1 \geq \lambda_2 \geq 0. \tag{57}$$

Averaging over the two eigenvalues gives

$$E\left[\hat{\boldsymbol{v}}(1)^\dagger \boldsymbol{H}(1)^\dagger \boldsymbol{H}(1) \hat{\boldsymbol{v}}(1)\right] = \int_0^\infty \int_0^{\lambda_1} \left(\lambda_1 - \frac{\lambda_1 - \lambda_2}{2^{BK}+1}\right) f_{\boldsymbol{\Lambda}}(\lambda_1, \lambda_2)\, \mathrm{d}\lambda_2 \mathrm{d}\lambda_1 \tag{58}$$

$$= 3.5 - \frac{3}{2^{BK}+1}. \tag{59}$$

Since $\boldsymbol{W}(k-i)$ and $\hat{\boldsymbol{v}}(1)$ are independent and $E[\boldsymbol{W}(k-i)^\dagger \boldsymbol{W}(k-i)] = 2\boldsymbol{I}$, we have that

$$E\left[\hat{\boldsymbol{v}}(1)^\dagger \boldsymbol{W}(k-i)^\dagger \boldsymbol{W}(k-i) \hat{\boldsymbol{v}}(1)\right] = E\left[2\hat{\boldsymbol{v}}(1)^\dagger \hat{\boldsymbol{v}}(1)\right] = 2. \tag{60}$$

We note that for general $\boldsymbol{W}$ whose size is $N_r \times N_t$, (60) can be generalized to

$$E\left[\hat{\boldsymbol{v}}(1)^\dagger \boldsymbol{W}(k-i)^\dagger \boldsymbol{W}(k-i) \hat{\boldsymbol{v}}(1)\right] = N_r. \tag{61}$$

Finally, we substitute (59) and (60) into (53) and simplify to obtain (11).

B. Proof of Lemma 2

We follow the derivation of $E\left[\hat{\boldsymbol{v}}(1)^\dagger \boldsymbol{H}(1)^\dagger \boldsymbol{H}(1) \hat{\boldsymbol{v}}(1)\right]$ for 2×2 channels in Appendix A and obtain the following expression for $2 \times N_r$ channels,

$$E\left[\hat{\boldsymbol{v}}(1)^\dagger \boldsymbol{H}(1)^\dagger \boldsymbol{H}(1) \hat{\boldsymbol{v}}(1)\right] = \int_0^\infty \int_0^{\lambda_1} \left(\lambda_1 - \frac{\lambda_1 - \lambda_2}{2^{BK}+1}\right) f_{\boldsymbol{\Lambda}}(\lambda_1, \lambda_2)\, \mathrm{d}\lambda_1 \mathrm{d}\lambda_2 \tag{62}$$

where $f_{\boldsymbol{\Lambda}}(\lambda_1, \lambda_2)$ is a joint pdf for the two ordered eigenvalues of a Wishart matrix $\boldsymbol{H}(1)^\dagger \boldsymbol{H}(1)$ given by [28]

$$f_{\boldsymbol{\Lambda}}(\lambda_1, \lambda_2) = \frac{\lambda_1^{N_r-2} \lambda_2^{N_r-2} (\lambda_1 - \lambda_2)^2 \mathrm{e}^{-(\lambda_1+\lambda_2)}}{(N_r-1)!(N_r-2)!}, \quad \lambda_1 \geq \lambda_2 \geq 0. \tag{63}$$

Note that we obtain the joint pdf in (57) by setting $N_r = 2$. Suppose

$$\phi(m,n) \triangleq \int_0^\infty \lambda_1^m \mathrm{e}^{-\lambda_1} \int_0^{\lambda_1} \lambda_2^n \mathrm{e}^{-\lambda_2}\, \mathrm{d}\lambda_2 \mathrm{d}\lambda_1, \quad \forall m,n \geq 1. \tag{64}$$

By substituting (63) into (62) and rearranging the terms, we can write $E\left[\hat{\boldsymbol{v}}(1)^\dagger \boldsymbol{H}(1)^\dagger \boldsymbol{H}(1)\hat{\boldsymbol{v}}(1)\right]$ in (62) in terms of $\phi(\cdot,\cdot)$ as shown in (16).

To evaluate (64), we apply integration by parts to the inner integral to obtain

$$\phi(m,n) = n\int_0^\infty \lambda_1^m \mathrm{e}^{-\lambda_1} \int_0^{\lambda_1} \lambda_2^{n-1} \mathrm{e}^{-\lambda_2}\, \mathrm{d}\lambda_2 \mathrm{d}\lambda_1 - \int_0^\infty \lambda_1^{m+n} \mathrm{e}^{-2\lambda_1}\, \mathrm{d}\lambda_1 \tag{65}$$

$$= n\int_0^\infty \lambda_2^{n-1} \mathrm{e}^{-\lambda_2} \int_{\lambda_2}^\infty \lambda_1^m \mathrm{e}^{-\lambda_1}\, \mathrm{d}\lambda_1 \mathrm{d}\lambda_2 - \frac{(m+n)!}{2^{m+n+1}} \tag{66}$$

where in (65), we switch the order of integration for the first integral and evaluate the second integral. We again evaluate the inner integral in (66) and switch the order of integration to obtain

$$\phi(m,n) = mn \underbrace{\int_0^\infty \lambda_1^{m-1} \mathrm{e}^{-\lambda_1} \int_0^{\lambda_1} \lambda_2^{n-1} \mathrm{e}^{-\lambda_2}\, \mathrm{d}\lambda_2 \mathrm{d}\lambda_1}_{\phi(m-1,n-1)} + \frac{m(m+n-1)!}{2^{m+n}} - \frac{(m+n)!}{2^{m+n+1}}. \tag{67}$$

Adding the last two terms in (67) gives (17). The initial conditions are obtained by evaluating the double integral in (64).

C. Proof of Lemma 3

Since the considered channel covariance $\boldsymbol{H}(1)^\dagger \boldsymbol{H}(1)$ has rank 2,

$$\lambda_3 = \lambda_4 = \cdots = \lambda_{N_t} = 0. \tag{68}$$

Applying the results from [25, eq. (18)], we obtain in Lemma 3 the expression for the cdf $F_{\boldsymbol{v}^\dagger \boldsymbol{\Lambda} \boldsymbol{v}}(x)$ for $\lambda_2 \leq x \leq \lambda_1$ only. Next we derive the expression of the cdf when $0 \leq x \leq \lambda_2$. The derivation is inspired by [29] where evaluating the cdf $F_{\boldsymbol{v}^\dagger \boldsymbol{\Lambda} \boldsymbol{v}}(x)$ was formulated as finding the surface area of an N_t-dimensional spherical cap. The results in [29] apply when $\boldsymbol{\Lambda}$ is full rank. In our case, $\boldsymbol{\Lambda}$ has rank 2 with nonzero diagonal entries λ_1 and λ_2.

Recall that $\boldsymbol{v} = [v_1 \ v_2 \ \cdots \ v_{N_t}]^T$ is an $N_t \times 1$ isotropically distributed vector with unit norm. Therefore, we have

$$\Pr\{\boldsymbol{v}^\dagger \boldsymbol{\Lambda}\ \boldsymbol{v} \geq x\} = \Pr\left\{\lambda_1 |v_1|^2 + \lambda_2 |v_2|^2 \geq x, \sum_{i=1}^{N_t} |v_i|^2 = 1\right\}. \tag{69}$$

In N_t-dimensional space, we can view the set of vectors $\{\boldsymbol{v} \in \mathbb{C}^{N_t} | \sum_{i=1}^{N_t} |v_i|^2 = 1\}$ as a surface of an N_t-dimensional unit ball centered at the origin. We can rearrange $\lambda_1|v_1|^2 + \lambda_2|v_2|^2 \geq x$ as follows

$$\frac{|v_1|^2}{\frac{x}{\lambda_1}} + \frac{|v_2|^2}{\frac{x}{\lambda_2}} \geq 1. \tag{70}$$

The above inequality describes the region outside a two-dimensional ellipse centered at the origin. Since $\lambda_1 \geq \lambda_2$, the widest part of the ellipse is determined by $\frac{x}{\lambda_2}$. Since we consider the regime where $0 \leq x \leq \lambda_2$ or $0 \leq \frac{x}{\lambda_2} \leq 1$, geometrically, the ellipse is completely contained in the N_t-dimensional unit ball.

We take the same analytical approach as the one in [29] by first finding the volume of the N_t-dimensional object prescribed by $\lambda_1|v_1|^2 + \lambda_2|v_2|^2 \geq x$ and $\sum_{i=1}^{N_t} |v_i|^2 \leq r^2$ where $r \geq 1$. (In the final steps, we will set $r = 1$.) Then, we compute its surface area, which is shown to be proportional to the desired cdf $F_{\boldsymbol{v}^\dagger \boldsymbol{\Lambda} \boldsymbol{v}}(x)$ [29].

The volume of the region $\{\boldsymbol{v} \in \mathbb{C}^{N_t} | \lambda_1|v_1|^2 + \lambda_2|v_2|^2 \geq x, \|\boldsymbol{v}\|^2 \leq r^2\}$ is denoted by

$$\begin{aligned}\mathsf{Vol}(\lambda_1|v_1|^2 + \lambda_2|v_2|^2 \geq x, \|\boldsymbol{v}\|^2 \leq r^2) &= \mathsf{Vol}(\|\boldsymbol{v}\|^2 \leq r^2) \\ &\quad - \mathsf{Vol}(\lambda_1|v_1|^2 + \lambda_2|v_2|^2 \leq x, \|\boldsymbol{v}\|^2 \leq r^2) \quad (71)\end{aligned}$$

where the volume of an N_t-dimensional ball with radius r is given by [29]

$$\mathsf{Vol}(\|\boldsymbol{v}\|^2 \leq r^2) = \frac{\pi^{N_t} r^{2N_t}}{\Gamma(N_t + 1)} \tag{72}$$

and $\mathsf{Vol}(\lambda_1|v_1|^2 + \lambda_2|v_2|^2 \leq x, \|\boldsymbol{v}\|^2 \leq r^2)$ is the volume of the ellipsoid that is completely contained in the hyperball with radius r.

To compute the volume of the ellipsoid, we first apply the following transformation

$$v_i = r_i \mathrm{e}^{j\theta_i}, \quad \forall i \tag{73}$$

where r_i and θ_i are the magnitude and phase of v_i, respectively. Using spherical coordinates, the volume of the ellipsoid is given by

$$\begin{aligned}&\mathsf{Vol}(\lambda_1|v_1|^2 + \lambda_2|v_2|^2 \leq x, \|\boldsymbol{v}\|^2 \leq r^2) \\ &= (2\pi)^{N_t} \int_{r_1=0}^{\sqrt{\frac{x}{\lambda_1}}} \int_{r_2=0}^{\sqrt{\frac{x-\lambda_1 r_1^2}{\lambda_2}}} \left(\int \cdots \int_{\sum_{n=3}^{N_t} r_n^2 \leq r^2 - r_1^2 - r_2^2} r_3 \cdots r_{N_t} \, \mathrm{d}r_3 \cdots \mathrm{d}r_{N_t} \right) r_1 r_2 \, \mathrm{d}r_2 \mathrm{d}r_1. \quad (74)\end{aligned}$$

We note that the multiple integral in the brackets in (74) is the volume of an $(N_t - 2)$-dimensional ball with radius $r^2 - r_1^2 - r_2^2$. Applying (72), we have

$$\begin{aligned}&\mathsf{Vol}(\boldsymbol{v}^\dagger \boldsymbol{\Lambda} \ \boldsymbol{v} \leq x, \|\boldsymbol{v}\|^2 \leq r^2) \\ &\qquad = \frac{(2\pi)^2 \pi^{N_t - 2}}{\Gamma(N_t - 1)} \int_{r_1=0}^{\sqrt{\frac{x}{\lambda_1}}} \int_{r_2=0}^{\sqrt{\frac{x-\lambda_1 r_1^2}{\lambda_2}}} r_1 r_2 (r^2 - r_1^2 - r_2^2) \, \mathrm{d}r_2 \mathrm{d}r_1 \quad (75) \\ &\qquad = \frac{\lambda_2}{2N_t(\lambda_1 - \lambda_2)} \left(\left(r^2 - \frac{x}{\lambda_1} \right)^{N_t} - \left(r^2 - \frac{x}{\lambda_2} \right)^{N_t} \right). \quad (76)\end{aligned}$$

To compute the surface area of the volume, we differentiate the volume as follows

$$\mathsf{Area}(\boldsymbol{v}^\dagger \boldsymbol{\Lambda}\ \boldsymbol{v} \leq x, \|\boldsymbol{v}\|^2 \leq 1) = \frac{\partial}{\partial x \partial r^2} \mathsf{Vol}(\boldsymbol{v}^\dagger \boldsymbol{\Lambda}\ \boldsymbol{v} \leq x, \|\boldsymbol{v}\|^2 \leq r^2)\bigg|_{r^2=1} \tag{77}$$

$$= \frac{\pi^{N_t}}{(N_t-2)!(\lambda_1-\lambda_2)} \left(\left(1-\frac{x}{\lambda_2}\right)^{N_t-2} - \left(1-\frac{x}{\lambda_1}\right)^{N_t-2} \right). \tag{78}$$

The surface area of the N_t-dimensional unit ball is given by

$$\mathsf{Area}(\|\boldsymbol{v}\|^2 \leq 1) = \frac{\partial}{\partial r^2} \mathsf{Vol}(\|\boldsymbol{v}\|^2 \leq r^2)\bigg|_{r^2=1} \tag{79}$$

$$= \frac{\pi^{N_t} N_t}{\Gamma(N_t+1)}. \tag{80}$$

The pdf of $\boldsymbol{v}^\dagger \boldsymbol{\Lambda} \boldsymbol{v}$ is given by [25, eq. (115)]

$$f_{\boldsymbol{v}^\dagger \boldsymbol{\Lambda} \boldsymbol{v}}(x) = -\frac{\mathsf{Area}(\boldsymbol{v}^\dagger \boldsymbol{\Lambda}\ \boldsymbol{v} \leq x, \|\boldsymbol{v}\|^2 \leq 1)}{\mathsf{Area}(\|\boldsymbol{v}\|^2 \leq 1)} \tag{81}$$

$$= \frac{N_t-1}{\lambda_1-\lambda_2} \left(\left(1-\frac{x}{\lambda_1}\right)^{N_t-2} - \left(1-\frac{x}{\lambda_2}\right)^{N_t-2} \right). \tag{82}$$

Finally, the cdf in (25) can be obtained by integrating the pdf in (82).

REFERENCES

[1] W. Santipach and K. Mamat, "Optimal feedback interval for temporally-correlated multiantenna channel," in *Proc. IEEE Global Telecommun. Conf. (GLOBECOM)*, Houston, Texas, USA, Dec 2011, pp. 1–5.

[2] İ. E. Telatar, "Capacity of multi-antenna Gaussian channels," *European Trans. on Telecommun.*, vol. 10, pp. 585–595, Nov. 1999.

[3] G. J. Foschini and M. J. Gans, "On limits of wireless communications in a fading environment when using multiple antennas," *Wireless Personal Commun.*, vol. 6, no. 3, pp. 311–335, Mar. 1998.

[4] D. J. Love, R. W. Heath, Jr., V. K. N. Lau, D. Gesbert, B. D. Rao, and M. Andrews, "An overview of limited feedback wireless communication systems," *IEEE J. Sel. Areas Commun.*, vol. 26, no. 8, pp. 1341–1365, Oct. 2008.

[5] W. Santipach and M. L. Honig, "Optimization of training and feedback overhead for beamforming over block fading channels," *IEEE Trans. Inf. Theory*, vol. 56, no. 12, pp. 6103–6115, Dec. 2010.

[6] ——, "Capacity of a multiple-antenna fading channel with a quantized precoding matrix," *IEEE Trans. Inf. Theory*, vol. 55, no. 3, pp. 1218–1234, Mar. 2009.

[7] D. J. Love and R. W. Heath, Jr., "Grassmannian beamforming for multiple-input multiple-output wireless systems," *IEEE Trans. Inf. Theory*, vol. 49, no. 10, pp. 2735–2745, Oct. 2003.

[8] W. Santipach and K. Mamat, "Tree-structured random vector quantization for limited-feedback wireless channels," *IEEE Trans. Wireless Commun.*, vol. 10, no. 9, pp. 3012–3019, Sep. 2011.

[9] Y. Ma, D. Zhang, A. Leith, and Z. Wang, "Error performance of transmit beamforming with delayed and limited feedback," *IEEE Trans. Wireless Commun.*, vol. 8, no. 3, pp. 1164–1170, Mar. 2009.

[10] B. Mondal and R. W. Heath, Jr., "Channel adaptive quantization for limited feedback MIMO beamforming systems," *IEEE Trans. Signal Process.*, vol. 54, no. 12, pp. 4717–4729, Dec. 2006.

[11] J. Choi, B. Clerckx, N. Lee, and G. .Kim, "A new design of polar-cap differential codebook for temporally/spatially correlated MISO channels," *IEEE Trans. Wireless Commun.*, vol. 11, no. 2, pp. 703–711, Feb. 2012.

[12] K. Huang, R. W. Heath, Jr., and J. G. Andrews, "Limited feedback beamforming over temporally-correlated channels," *IEEE Trans. Signal Process.*, vol. 57, no. 5, pp. 1–18, May 2009.

[13] T. Kim, D. J. Love, and B. Clerckx, "Does frequent low resolution feedback outperform infrequent high resolution feedback for multiple antenna beamforming systems?" *IEEE Trans. Signal Process.*, vol. 59, no. 4, pp. 1654–1669, Apr. 2011.

[14] A. Osmane and H. Khanfir, "Optimal feedback updating period for coordinated multi-point transmission schemes," in *Proc. IEEE Int. Symp. on Personal, Indoor, and Mobile Radio Commun. (PIMRC)*, London, UK, Sep. 2013, pp. 2281–2285.

[15] L. Zhang, L. Song, M. Ma, and B. Jiao, "On the minimum differential feedback for time-correlated MIMO Rayleigh block-fading channels," *IEEE Trans. Commun.*, vol. 60, no. 2, pp. 411–420, Feb. 2012.

[16] J. Xu, F. Huang, and D. Ben, "Quantised innovation Kalman filter: Performance analysis and design of quantised level," *IET Signal Processing*, vol. 8, no. 7, pp. 759–773, Sep. 2014.

[17] O. Mehanna and N. D. Sidiropoulos, "Channel tracking and transmit beamforming with frugal feedback," *IEEE Trans. Signal Process.*, vol. 6, no. 24, pp. 6402–6413, Apr. 2014.

[18] S. Noh, M. D. Zoltowski, and D. J. Love, "Training sequence design for feedback assisted hybrid beamforming in massive MIMO systems," *IEEE Trans. Commun.*, vol. 64, no. 1, pp. 187–200, Jan. 2016.

[19] K. Mamat and W. Santipach, "On transmit beamforming for MISO-OFDM channels with finite-rate feedback," *IEEE Trans. Commun.*, vol. 63, no. 11, pp. 4202–4213, Nov. 2015.

[20] D. J. Love, R. W. Heath, Jr., W. Santipach, and M. L. Honig, "What is the value of limited feedback for MIMO channels?" *IEEE Commun. Mag.*, vol. 42, no. 10, pp. 54–59, Oct. 2004.

[21] Y. Zhao, M. Zhao, L. Xiao, and J. Wang, "Capacity of time-varying Rayleigh fading MIMO channels," in *Proc. IEEE Int. Symp. on Personal, Indoor and Mobile Radio Commun. (PIMRC)*, Berlin, Germany, Sep. 2005, pp. 547–551.

[22] C. B. Peel and A. L. Swindlehurst, "Throughput-optimal training for a time-varying multi-antenna channel," *IEEE Trans. Wireless Commun.*, vol. 6, no. 9, pp. 3364–3373, Sep. 2007.

[23] W. C. Jake, *Microwave Mobile Communication*. New York, NY, USA: IEEE Press, 1993.

[24] W. Dai, Y. Liu, and B. Rider, "The effect of finite rate feedback on CDMA signature optimization and MIMO beamforming vector selection," *IEEE Trans. Inf. Theory*, vol. 55, no. 8, pp. 3651–3669, Aug. 2009.

[25] V. Raghavan and V. V. Veeravalli, "Ensemble properties of RVQ-based limited-feedback beamforming codebooks," *IEEE Trans. Inf. Theory*, vol. 59, no. 12, pp. 8224–8249, Dec. 2013.

[26] A. M. Tulino and S. Verdú, "Random matrix theory and wireless communications," *Foundations and Trends in Communications and Information Theory*, vol. 1, no. 1, pp. 1–182, 2004. [Online]. Available: http://dx.doi.org/10.1561/0100000001

[27] S. P. Lloyd, "Least squares quantization in PCM," *IEEE Trans. Inf. Theory*, vol. 28, no. 2, pp. 129–136, Mar. 1982.

[28] R. A. Fisher, "The sampling distribution of some statistics obtained from non-linear equations," *Annals of Eugenics*, vol. 9, pp. 238–249, 1939.

[29] K. K. Mukkavilli, A. Sabharwal, E. Erkip, and B. Aazhang, "On beamforming with finite rate feedback in multiple antenna systems," *IEEE Trans. Inf. Theory*, vol. 49, no. 10, pp. 2562–2579, Oct. 2003.